

## **NICMOS Software: An Observation Case Study**

E. Stobie, D. Lytle, A. Ferro and I. Barg

*University of Arizona, Steward Observatory, NICMOS, Tucson, AZ  
85721*

**Abstract.** The Near Infrared Camera and MultiObject Spectrometer (NICMOS) was installed on the Hubble Space Telescope during the Second Servicing Mission in February, 1997. NICMOS Proposal 7111, the imaging of Orion OMC-1, was selected as an Early Release Observation (ERO) to be executed in the Science Mission Observatory Verification (SMOV) period shortly afterwards. Calibration and analysis of this observation posed very interesting challenges for the authors, in particular dealing with an exciting new instrument whose on-orbit calibration was not yet well defined.

### **1. Introduction**

NICMOS contains three cameras with adjacent, but not spatially contiguous fields-of-view of 11, 19.2, and 51.2 arcseconds which provide infrared imaging and spectroscopic observations that cover the spectral range of 0.8 to 2.5 microns. Proposal 7111 imaged the core of OMC-1 using the NICMOS high and intermediate resolution cameras with seven 160-second exposures, composed of 13 non-destructive reads (multiaccum mode) for both the F212N and F215N filters. Five mosaic positions were observed during five consecutive orbits as well as observations for dark and flat calibration. The purpose of the observation was to resolve structure in the molecular hydrogen outflow close to the outflow source (or sources) in OMC-1.

Many steps were required to process the raw OMC-1 data into a final calibrated mosaiced image. Darks and flats had to be created from contemporaneous reference observations and problems within the calibration process had to be resolved. Mosaicing software had to be developed to create the final product.

### **2. Reference Files**

#### **2.1. Introduction**

The NICMOS chips present some interesting differences in the reference files which are used to generate calibrated data. Because the ability to do non-destructive reads of the chip and the associated electronics, as well as the materials used in construction of the chips, there are many differences between

reference data in the NICMOS chips and those found in normal CCD reductions.

## 2.2. Darks

*Special Considerations:* In addition to the dark current, similar to that found in CCDs, NICMOS dark frames are also used to remove several other systematic effects. These include the signature of the electronics, known as “shading”, and the contamination from the heat generated by the detector’s readout amplifiers, known as amp glow. Figure 1 shows a dark frame in which these signatures can be seen.

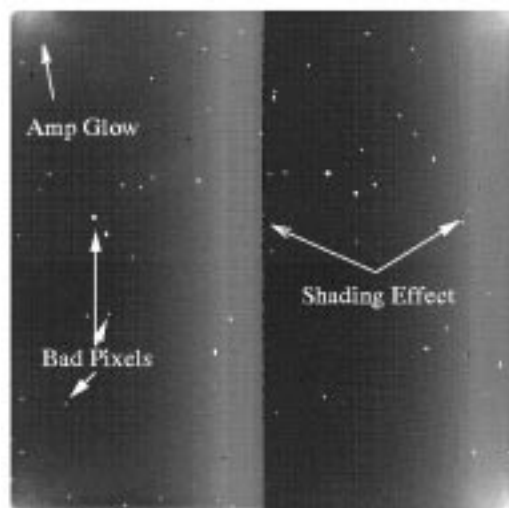


Figure 1. Dark with problem areas.

*How we generated the dark:* Application of the darks in calibration requires that the darks be treated as counts as opposed to count-rates. Also, darks must be applied to individual readouts of the detector. Each readout from a data sequence must have a corresponding dark readout.

Because the darks are combined in terms of individual readouts, normal NICMOS cosmic ray detection (noting a rapid increase in charge in a pixel), cannot be used. Instead a number of darks were taken and median combined. This produced a final dark series in which very few if any cosmic rays should be present. The final step in producing the dark used for calibration of the data was to recombine the individual readouts into a single file in the format required by the *CALNICA* program, an IDL procedure called *BuildRef*, software written by the authors.

## 2.3. Flats

*Special Considerations:* The NICMOS detectors have a large change in quantum efficiency across the chip. This results in a flat field which has a great deal of structure. One problem with this data set is that the filters used, 212N and 215N are quite narrow, which means that a well exposed flat frame was difficult

to obtain. In the NICMOS instrument, flat fields are generated by observing a blank part of the sky and illuminating one of the optical elements with a flat field illuminator. Care must be taken that the observed sky does not contain any strong sources.

*How we generated the flats:* The flat fields were generated by running the data through normal processing with *CALNICA* up to the point of removing the flat field. This included subtraction of the zeroth read, dark subtraction and cosmic ray rejection. The images were median combined to increase signal to noise and to obtain a single flat image.

### 3. Calibrating the Data

#### 3.1. Introduction

The calibration process using *CALNICA* was straightforward once the headers of the raw images were edited to use our newly created reference darks and flats. However, it became obvious that there were problems in the the linearity correction and in the detection of saturated pixels that led to poor cosmic ray detection.

#### 3.2. Repairing the Zeroth Read

When observing very bright sources with NICMOS (the central object, BN, is approximately 5th magnitude), signal from the object may appear in the zeroth read (bias frame). This results in too much bias being subtracted from all of the subsequent reads causing pixels to fall on an incorrect location on the non-linearity curve. In extreme cases the data may be saturated by the first readout.

We compared the zeroth read of each observation with a super bias frame from a large set of dark observations. Where the value in the zeroth read deviated by more than 5 sigma from the super bias value, the pixel value was replaced with the super bias value (procedure *satfix*). No pixels were shown to be approaching saturation by the first read, i.e., the difference between a value in the zeroth read and the super bias image is greater than 12,000 ADU.

#### 3.3. Detecting Saturated Pixels

During the cosmic ray rejection step of the calibration process many pixels were flagged as containing cosmic rays when they were actually saturated. This caused a bad fit across the readouts and a poor value for the pixel in the final image. The problem was that a substantial number of pixels in the saturation node of the nonlinearity reference file were defined too high. (Pixels that depart by more than 6% from linearity are considered saturated and unusable.) Since very little on-orbit linearity/saturation calibration data had been taken to date, we used the solution suggested by STScI, i.e., adjust all values in the saturation node downward by 9%. With this change to the saturation node values all saturated pixels were properly detected.

#### 4. Creating the Mosaiced Image

The five positions surrounding BN were observed without the use of a dither pattern and the orientation varied from the exposure on one position to another so that they could not be processed through the STScI CALNICB step of the pipeline. We developed an interactive mosaic task, *NICMosaic*, to combine the images together. Figure 2 shows the mosaic image created by *NICMosaic*.

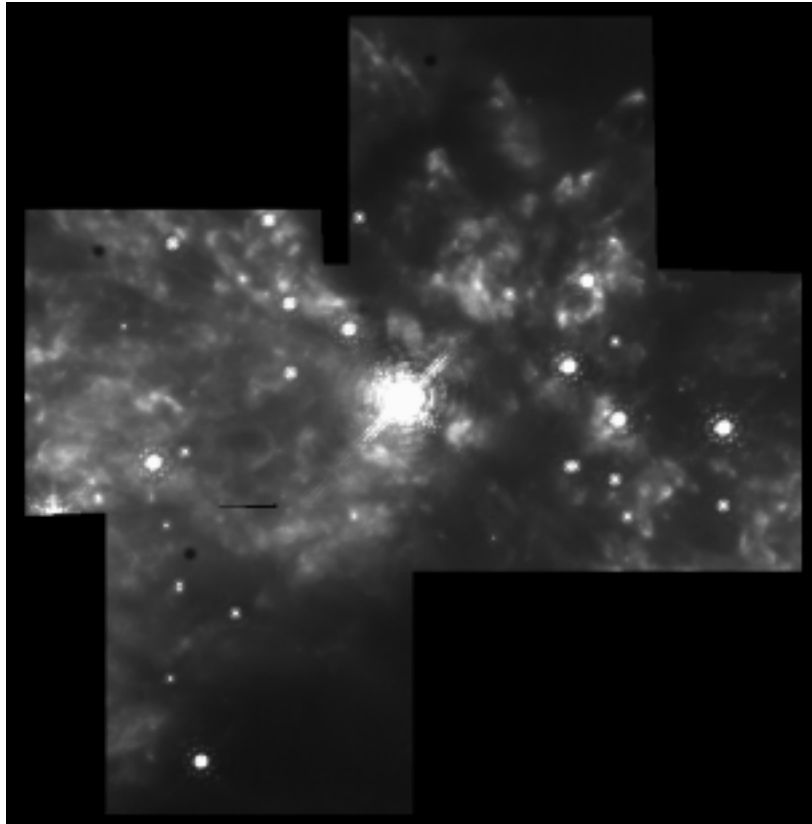


Figure 2. Mosaic of OMC-1.

#### 5. Summary:

The primary obstacles in the reduction were due to the unique aspects of the NICMOS detectors, as well as the new, more complex, format of the data from HST. Once these factors are understood, the reduction and analysis of NICMOS data is straightforward.

**Acknowledgments.** We would like to thank Ed Erickson and Susan Stolovy for allowing us to use their ERO data in this paper. We also appreciate many discussions with Susan regarding the analysis of the data.